

## Magnetic excitations in the dilute anisotropic antiferromagnet $\text{Fe}_x\text{Zn}_{1-x}\text{F}_2$

C. Paduani,\* D. P. Belanger, J. Wang, and S-J. Han

*Physics Department, University of California, Santa Cruz, California 95064*

R. M. Nicklow

*Solid State Division, Oak Ridge National Laboratory, Oak Ridge, Tennessee 37831*

(Received 22 October 1993; revised manuscript received 6 January 1994)

We have measured magnetic excitations in dilute crystals of the three-dimensional anisotropic antiferromagnet  $\text{Fe}_x\text{Zn}_{1-x}\text{F}_2$  with  $x=0.69, 0.59,$  and  $0.31$  using inelastic-neutron-scattering techniques. Well-defined spin excitations at the higher concentrations are not observed above the transition temperature. A magnetic excitation spectrum with significant structure is observed at low temperature. In the case of  $x=0.59$ , we observe three nearly dispersionless intensity peaks in the energy scans. The lowest-energy peak dominates near the zone center. The three energy peaks become comparable in intensity as the zone boundary is approached. The structure in the peaks, if measured under conditions of low instrumental resolution, could appear as damping away from the zone center, consistent with the behavior reported previously for the similar but less anisotropic system  $\text{Mn}_{0.5}\text{Zn}_{0.5}\text{F}_2$ , where the apparent damping has been identified with "fracton" effects. We argue that such an interpretation is, for the most part, inappropriate for  $\text{Fe}_x\text{Zn}_{1-x}\text{F}_2$  for  $x \geq 0.31$ , where the percolation threshold is  $x_p=0.24$ , and highly questionable for the  $\text{Mn}_{0.5}\text{Zn}_{0.5}\text{F}_2$  system.

### I. INTRODUCTION

Randomly dilute Ising antiferromagnetics have been extensively investigated for a number of years and the highly anisotropic antiferromagnetic system  $\text{Fe}_x\text{Zn}_{1-x}\text{F}_2$  has proven to be a model three-dimensional system. Well above the percolation threshold ( $x \gg x_p=0.24$ ) in zero applied field,  $\text{Fe}_x\text{Zn}_{1-x}\text{F}_2$  is an excellent example of the random-exchange Ising model. With a field applied along the spin ordering axis the same system becomes an archetypal random-field Ising model system.<sup>1-3</sup> Near the percolation threshold, for  $0.24 \leq x \leq 0.31$ , the system displays many spin-glasslike features<sup>4</sup> associated with slow Ising percolation threshold dynamics<sup>5</sup> although the system is not a canonical spin glass,<sup>6</sup> since it lacks any significant exchange frustration. The statics and dynamics of these models or randomness have been extensively studied using this ideal system. Less work has been done with the aim of understanding the excitation spectra in three-dimensional dilute Ising systems at low temperature. We address the latter topic in the present work using the highly characterized  $\text{Fe}_x\text{Zn}_{1-x}\text{F}_2$  system.

The focus of some previous experimental work and much of the theoretical efforts on the low-temperature excitations in less anisotropic systems has been directed to fracton excitations which are expected on a fractal lattice near the percolation threshold.<sup>7-12</sup> A site-dilute antiferromagnet is a model example of a percolation network near the percolation threshold, particularly when essentially only one magnetic interaction exists, as in the case of  $\text{Fe}_x\text{Zn}_{1-x}\text{F}_2$ . If the anisotropy is not too large, a crossover from long-range magnon excitations to short-range fracton excitations is expected.<sup>12</sup> Hence, one might anticipate fracton effects in the excitation spectrum, but

only very close to the percolation threshold. A report of an observation of such a crossover has been made<sup>11</sup> in  $\text{Mn}_{0.5}\text{Zn}_{0.5}\text{F}_2$  which, except for a smaller anisotropy, is almost identical to  $\text{Fe}_x\text{Zn}_{1-x}\text{F}_2$  in its magnetic properties. However, although the concentration  $x=0.5$  maximizes the randomness of the magnetic site occupation, this concentration is very far above the percolation threshold,  $x_p=0.24$ , and fracton behavior could be very difficult to observe. Furthermore, the anisotropy in this system is significant, so the theoretical models based on fractons in the isotropic Heisenberg model may have limited applicability.<sup>7,12</sup> There has not been a systematic study of  $\text{Mn}_x\text{Zn}_{1-x}\text{F}_2$  for concentrations closer to the percolation threshold. Alternative explanations for the observed behavior of  $\text{Mn}_{0.5}\text{Zn}_{0.5}\text{F}_2$  should be considered. In elucidating the character of the low-temperature excitations, it is useful to examine the excitation spectrum in an even more anisotropic magnet such as  $\text{Fe}_x\text{Zn}_{1-x}\text{F}_2$ . To do this, we have used three  $\text{Fe}_x\text{Zn}_{1-x}\text{F}_2$  crystals to investigate how the low-temperature excitations evolve in anisotropic diluted antiferromagnets as the concentration is reduced toward the percolation threshold.

### II. PRELIMINARY DETAILS

Inelastic neutron-scattering experiments were performed using the triple-axis spectrometer HB2 at the High Flux Isotope Reactor at the Oak Ridge National Laboratory, on crystals of  $\text{Fe}_x\text{Zn}_{1-x}\text{F}_2$ . Using the concentrations  $x=0.69, 0.59,$  and  $0.31$ , we were able to observe the characteristics of excitations far above and close to the percolation threshold  $x_p=0.24$ . The crystal sizes were typically a few millimeters in each direction. The lattice parameters for these crystals are approximately

4.7 Å for the  $a$  and  $b$  axes and 3.2 Å for the  $c$  axis. The transition temperatures are  $T_N = 54.1, 46.3,$  and  $19.8$  K for  $x = 0.69, 0.59,$  and  $0.31,$  respectively. The two higher concentration crystals were oriented with the  $c$ -axis vertical to the horizontal scattering plane. The third crystal was aligned with an  $a$ -axis vertical. The latter crystal was actually twinned, with two comparable crystallites rotated by approximately  $5^\circ$ . We were able to align one part of the twinned crystal and the measurements should not have been significantly affected by the second crystallite, since the misalignment is relatively large compared to the instrumental resolution parameters and, although the second crystallite may contribute at a different  $q$  than the primary one, the dispersion in this crystal was found to be negligible. For most of the measurements, a pyrolytic graphite monochromator and analyzer were used with the final neutron energy fixed at 14.8 meV. Two different sets of collimations were used. The first was 60 min of arc before the monochromator, 40 between monochromator and sample, 40 between the sample and analyzer, and 70 between the analyzer and detector yielding a full width at half maximum (FWHM) energy resolution of 1.6 meV. The second was with the corresponding divergences of 60, 20, 20, and 70 minutes of arc yielding a

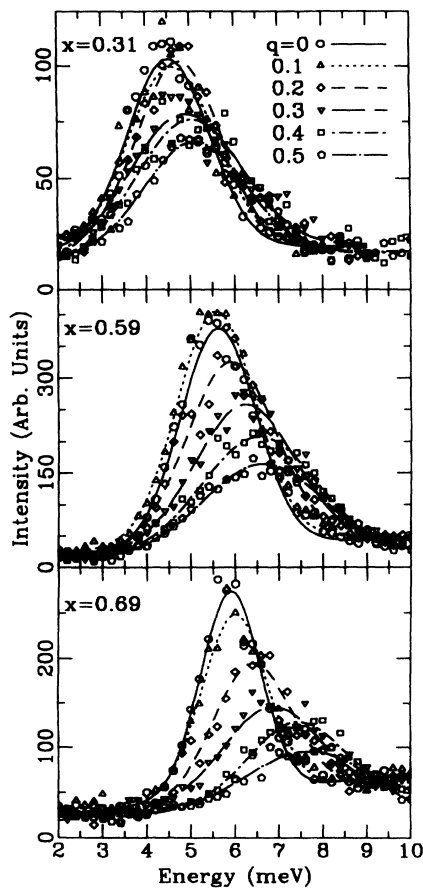


FIG. 1. The low-temperature scattering intensity vs energy for  $x = 0.31, 0.59,$  and  $0.69$  for several values of  $q$ . For  $x = 0.31$  the data are from  $(1, 0, -q)$  scans. For  $x = 0.59$  and  $0.69$  data,  $(1, -q, 0)$  scans are shown. The curves are Gaussian fits to the data.

FWHM of approximately 1.1 meV. All of the results used in Figs. 1–3 were obtained using the coarser resolution. For the high-resolution measurements on the  $x = 0.59$  crystal, the final energy was set at 6.5 meV and most of the data were taken with collimations of 50, 40, 80, and 120 min of arc, respectively, providing a FWHM of approximately 0.65 meV. A pyrolytic graphite filter was used in all cases to remove contamination from higher-energy neutrons.

The three-dimensional Ising antiferromagnet  $\text{FeF}_2$  has a rutile structure with the magnetic ions forming a body-centered tetragonal lattice. The magnetic interactions are very well modeled<sup>13</sup> by the Hamiltonian

$$H = J_2 \sum_{\langle i,j \rangle} \mathbf{S}_i \cdot \mathbf{S}_j - D \sum_i (S_i^z)^2, \quad (1)$$

with  $J_2 = 0.435$  meV and  $D = 0.861$  meV, where the sum

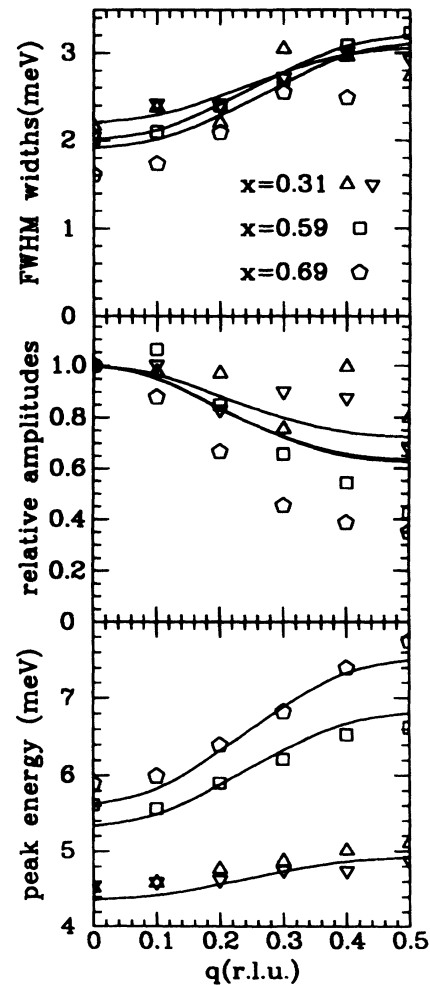


FIG. 2. The line-shape widths, relative amplitudes and energies of the excitations obtained by fitting the experimental data to Gaussian line shapes for  $x = 0.31, 0.59,$  and  $0.69$  vs  $q$ . The curves are obtained by fitting the cluster model results with a Gaussian line shape, with no adjustable parameters, as described in the text. For  $x = 0.31$ , the upward pointing triangles are for  $(1, 0, -q)$  scans and the downward triangles are for  $(-q, 0, 1)$  scans. The  $(0, 0, 1+q)$  scans yields the same results within experimental error.

is over second-nearest neighbors only. The corresponding exchange field is 54.8 T, the strong single-ion uniaxial anisotropy field is 19.2 T, and the Néel temperature is  $T_N = 78.4$  K. The energy of magnons at the zone boundary is 9.56 meV, while the Ising gap at the zone center is 6.53 meV. The second-nearest-neighbor exchange interaction between the body-center and body-corner spins is predominant; the first- and third-neighbor interactions are negligible.

Wertheim, Buchanan, and Guggenheim<sup>14</sup> determined, using Mössbauer measurements, that the Néel temperature in the system  $\text{Fe}_x\text{Zn}_{1-x}\text{F}_2$  is proportional to the iron concentration for all concentrations  $x > 0.4$ . From experimental measurements of electronic transitions, a small linear increase of the magnetic anisotropy with zinc dilution was deduced in addition to a linear decrease of the exchange field by de Araujo.<sup>15</sup> Upon dilution the antiferromagnetic exchange interaction between the next-nearest-neighbor ions continues to be much larger than those between first- and third-neighbor ions.<sup>16</sup>

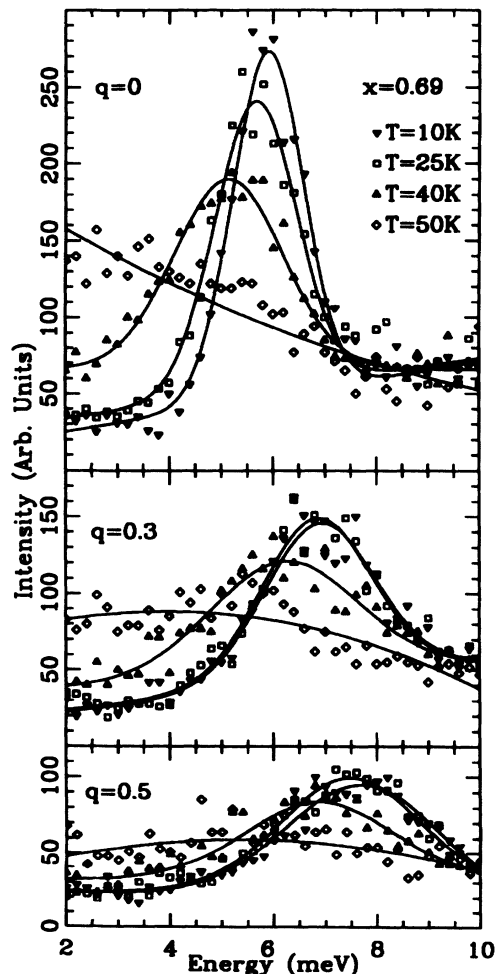


FIG. 3. The scattering intensity vs energy for  $x=0.69$  at various temperatures and  $q=0, 0.3, \text{ and } 0.5$  rlu. The transition temperature is  $T = 54.1$  K.

### III. EXPERIMENTAL RESULTS AND DISCUSSION

We first discuss the measurements obtained using the low-resolution spectrometer configurations. Neutron scattering profiles were obtained at temperatures  $T=10, 25, 40, \text{ and } 50$  K for  $x=0.69$ , at  $T=12, 24, 33, \text{ and } 38$  K for  $x=0.59$  and at  $T=11$  and  $15$  K for  $x=0.31$ . The constant- $q$  measurements were performed for  $(1, 0, -q)$ ,  $(-q, 0, 1)$ , and  $(0, 0, 1+q)$  for  $x=0.31$  and for  $(1, -q, 0)$  for  $x=0.59$  and  $0.69$ , where  $q$  ranged from the zone center ( $q=0$ ), to the zone boundary [ $q=0.5$  reduced lattice units (rlu)].

Typical scattering profiles are shown in Fig. 1 at the lowest temperatures for each sample. The curves are fits of the data to simple Gaussian line shapes. Fits were also made to damped harmonic oscillator line shapes with the instrumental resolution folded in, since such a profile has been employed previously.<sup>17</sup> However, the fit quality and informational content are essentially the same as with the fits depicted in Fig. 1 and none of the conclusions drawn from the analysis depend upon which fitting function is used. Both fits allow for a constant background term. In these measurements, no attempt has been made to determine if the background contribution has any small magnetic component. We do not intend to imply that either the Gaussian or damped harmonic oscillator expressions is correct for a physical description of the inelastic scattering. In fact, we will show later that neither is appropriate for the detailed analysis, since fine structure has been observed with a higher resolution spectrometer configuration. However, we find the Gaussian fits useful in the characterization of the gross features of the data. The Gaussian linewidths are shown in Fig. 2(a), the amplitudes in Fig. 2(b) and the peak energies in Fig. 2(c); all are plotted versus  $q$ . One can see clearly how the excitation energies tend to decrease with decreasing magnetic concentration, as expected. It is apparent also that the dispersion, as determined from the Gaussian fits, decreases as the concentration approaches the percolation threshold, indicating that the excitations are becoming more localized. Within experimental error, all three types of scan configurations for  $x=0.31$  yield the same results, indicating little dependence on whether  $q$  or  $Q$  are perpendicular or parallel to the spin ordering direction. The energy widths vary with  $q$  in a similar manner for all three crystals. The energy width for an overdamped mode should be comparable to the peak energy. For all cases in these measurements, the widths of the peaks are significantly less than the peak energies suggesting that these modes are not overdamped. This contrasts the behavior as interpreted in the  $\text{Mn}_x\text{Zn}_{1-x}\text{F}_2$  experiments.<sup>11</sup> A main distinguishing feature among the three samples is the degree to which the amplitude varies with  $q$ . The sample with the largest magnetic concentration,  $x=0.69$  shows the most dramatic decrease in the peak intensity with increasing  $q$ . The crystal with the smallest magnetic concentration ( $x=0.31$ ) shows little amplitude variation. The behavior of this system is not compatible with the interpretation given in the work<sup>11</sup> on the very similar, though less anisotropic system  $\text{Mn}_{0.5}\text{Zn}_{0.5}\text{F}_2$ . In that work, the data were described in

terms of a magnon at small  $q$  and an overdamped fracton excitation at large  $q$ . We observe no strong  $q$ -dependent damping in  $\text{Fe}_x\text{Zn}_{1-x}\text{F}_2$ , but the decrease in amplitude, if ascribed to fracton effects, would lead one to the paradoxical conclusion that the greatest fracton effect occurs for larger  $x$ . As we will show below, higher-resolution energy scans reveal structure, which precludes a simple fracton interpretation of the behavior of the  $\text{Fe}_x\text{Zn}_{1-x}\text{F}_2$  system.

To ensure that the energy scans shown in Fig. 1 are, in fact, representative of the lowest-temperature excitations without appreciable thermal broadening, we examined the temperature dependence of the profiles for all three crystals. An example is shown for  $x=0.69$  in Fig. 3 for  $T=10, 25, 40$  and  $50$  K. At the highest temperature, near the transition temperature  $T_N=54$  K, only a very broad magnetic excitation is observed. The excitation peaks become sharper as the temperature is reduced, but there is relatively little difference between the scans at the lowest two temperatures. This is true of each of the samples, indicating that the broad structure of the lowest-temperature scans is not substantially originating from thermal effects but instead from geometric randomness. Sharp excitations are not observed above the transition temperature in  $\text{Fe}_x\text{Zn}_{1-x}\text{F}_2$  at the two larger concentrations.

One of the simplest models used to describe magnetic excitations in disordered systems is the Ising "cluster" model.<sup>17</sup> This model actually has little to do with clusters of magnetic spins and is instead a model based on the local environments of individual spins. It is expected to be a reasonable approximation in anisotropic systems, particularly near the zone boundary. Specifically, the cluster model should not be applicable when long-wavelength excitations are involved. This model has been applied with some success<sup>18</sup> to  $\text{Co}_x\text{Zn}_{1-x}\text{F}_2$ . In accordance with previous<sup>15</sup> experimental results, we use a linear reduction of the exchange field with increasing zinc concentration and a linear increase of the magnetic anisotropy. We can accurately model the experimentally determined exchange and anisotropy for the diluted system using the phenomenological expressions

$$J = xJ_0 \quad (2)$$

and

$$D = (1 + (1-x)/6)D_0, \quad (3)$$

where  $J_0$  and  $D_0$  are the exchange and anisotropy parameters for pure  $\text{FeF}_2$ . The excitation frequencies are given by the expression

$$\omega_q^2 = (\omega_e + \omega_a)^2 - \omega_e^2 \cos(\pi q)^2, \quad (4)$$

where  $\hbar\omega_e = zSJ$ ,  $\hbar\omega_a = D(2S-1)$ , and  $S=2$ ; we use the discrete values  $J = (n/z)J_0$ ,  $D = [1 + (1-n/z)/6]D_0$ , with  $n$  the number of magnetic neighbors around particular  $\text{Fe}^{2+}$  ions. As mentioned above, this extension of the cluster model to  $q < 0.5$  is less valid than at the zone boundary, but provides some qualitative means for the characterization of the  $q$  dependence of the scattering

and can hint at the range of  $q$  for which local excitations are relevant.

Gaussian line shapes with widths equal to the instrumental energy resolution are located at the appropriate energies for each possible number of neighboring magnetic ions and the amplitudes are weighted by the probabilities

$$P(n) = \frac{z!}{n!(z-n)!} (1-x)^{z-n} (x)^n \quad (5)$$

for finding magnetic ions with  $n$  neighbors. The overall line shape is then constructed by summing the individual Gaussians, resulting in a smooth curve for the instrumental resolution used. The curves in Fig. 2 are the results for the widths, relative amplitudes and positions obtained by fitting one Gaussian line shape to the smooth composite line shape. The fits are quite good and the agreement for the widths and positions of the experimental and calculated line shapes is remarkable. This suggests that local configurations are indeed integral to the observed behavior. The only obvious discrepancy between the model and the low-resolution line shapes is found in the relative amplitudes. This quite possibly reflects the contribution to the data from magnon excitations at smaller  $q$ . The discrepancy decreases as  $x$  approaches  $x_p$ , since the system near  $x_p$  can less adequately support magnons. Despite the apparent success of the cluster model, the details of the energy spectrum cannot be described this simply, as we deduce from the higher-resolution data presented below.

Since the cluster model seems to be successful in describing the overall line widths and general shape of the excitations for all three samples at the resolution used in the initial experiments, particularly at the zone boundary, we attempted to observe fine structure associated with the individual cluster model excitations. We repeated the energy scans for the  $x=0.59$  sample using the finer instrumental energy resolution of  $0.65$  meV described above, which should be sufficient to partially resolve the cluster model peaks if they are resolution limited. The results of the measurements are shown in Fig. 4 for several values of  $q$ . Structure, in the form of three peaks, is observed in these scans and it changes with  $q$ . The solid curves in Fig. 4 are Gaussian fits to the data with FWHM equal to  $1.2$  meV. Fits to more than three peaks were not successful, although it is, of course, conceivable that small peaks do exist. The widths of the larger peaks, when allowed to vary, yielded the FWHM widths of approximately  $1.2$  meV. The three peak positions do not correspond to positions predicted by the cluster model. Instead, they have a much larger spacing, thereby filling the overall energy range spanned by the cluster model prediction, but with peaks separated widely enough to allow partial resolution of the peaks. The positions of the peaks do not change appreciably with  $q$ , whereas the relative amplitudes of the three peaks change considerably. We conclude that the intrinsic widths of the excitations are approximately  $1.2$  meV, since scans taken at higher-resolution yield comparable structure. Near the zone boundary, the three peaks are of comparable intensity. At the zone center nearly all of the scatter-

ing is contained in the lowest-energy peak. The residual peaks at the higher-energy positions may be largely a result of the finite-energy resolution. At the zone center, it is tempting to attribute the scattering to magnon excitations and at finite  $q$  to attribute the scattering at the higher-energy peaks to excitations that are localized in nature. The lowest-energy peak intensity may have a localized contribution, since it has a dispersionless component which survives at large  $q$ . The lack of dispersion of the peaks also points to a localized character. The apparent shifting of the peak positions with  $q$  in the low-resolution scans shown in Fig. 2 is attributable to the shift in spectral weight from the low-energy extended state to the localized states. This is in contradiction to the interpretation of the shift as indicating a crossover from a magnon to a damped fracton excitation, which

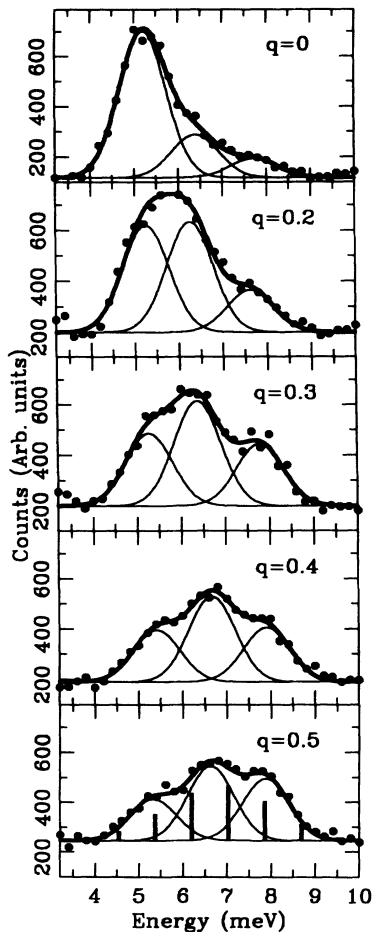


FIG. 4. High-resolution intensity vs  $q$  scans at various  $q$  for  $x=0.59$ . The light curves represent three Gaussian peaks used to fit the data. The dark curve is the sum of the three individual peaks. The  $q=0.5$  rlu data were obtained with slightly different spectrometer collimations and the intensities cannot be directly related to the other scans. Note that the intensity and energy axes do not extend to zero. The solid vertical line segments indicate the position and relative intensities for the cluster model excitations for  $q=0.5$ . The one with an energy just above 7 meV corresponds to five neighbors.

one might expect in an isotropic system very close to the percolation threshold.

There is at this time no theoretical understanding of the detailed nature of the observed peak structure in  $\text{Fe}_x\text{Zn}_{1-x}\text{F}_2$ . The only concrete prediction is a recent one of Korenblit and Shender,<sup>19</sup> who show that the ratio of the damping to the dispersion should increase in anisotropic systems as  $q$  decreases toward zero. Since the high-resolution peaks appear to have widths that are approximately twice the instrumental energy resolution, including at  $q=0$ , we may be observing the damping predicted by them.

#### IV. CONCLUSIONS

The description of the energy spectra in dilute, anisotropic  $\text{Fe}_x\text{Zn}_{1-x}\text{F}_2$  crystals cannot be made simply in terms of the crossover from a single long-wavelength excitation at the zone center to an overdamped fracton excitation as  $q$  is increased toward the zone boundary. Instead, the observed behavior is consistent with some other localized excitations for  $q>0$  and a magnon near  $q=0$ . The simple cluster model is adequate at describing the overall width and position of the spectra but fails to predict the predominance of the three main peaks at finite  $q$  observed for  $x=0.59$  with high resolution.

Recent experiments on a random, isotropic  $d=3$  system,  $\text{RbMn}_x\text{Mg}_{1-x}\text{F}_3$ , by Takahashi and Ikeda<sup>20</sup> show a similar lack of clear crossover from an extended state to a broad fracton excitation for  $x \gg x_p$ . They found essentially dispersionless peaks near the zone boundary with energies consistent with the six cluster model excitations corresponding to the six nearest-neighbor configurations. This is in some ways surprising, since it was thought that the cluster model would only be appropriate to the anisotropic case. Indeed, quantitative analysis of the relative intensities shows disagreement with the cluster model. Near the zone center, a predominant sharp energy peak associated with a propagating spin wave is observed as well as shoulders above and below the main peak. In the crossover region between these behaviors, two pronounced peaks and other smaller peaks were observed. In this isotropic system the cluster model excitations are widely separated, since the anisotropy contributions to the excitation energies are negligible.

In the anisotropic system  $\text{Rb}_2\text{Co}_x\text{Mg}_{1-x}\text{F}_4$ , for  $x < x_p$ , Ikeda and Ohoyama<sup>21</sup> found evidence for both peaks originating from intracenter excitations, which can be predicted by exact diagonalizations of the appropriate Hamiltonian, and thermal Ising cluster excitations over the entire range of concentrations. The excitations tend to be well separated, facilitating energy-peak resolution in the experiments. Exact diagonalization is not an appropriate approach to the present case of  $\text{Fe}_x\text{Zn}_{1-x}\text{F}_2$  for  $x \gg x_p$ .

From the results of the experiments on the  $d=3$  isotropic and  $d=2$  anisotropic antiferromagnets, one might expect the cluster model to be quite applicable well above  $x_p$  in an anisotropic  $d=3$  antiferromagnet. However, the three-peak structure with energy spacings inappropriate

to the cluster model observed in the  $\text{Fe}_{0.59}\text{Zn}_{0.41}\text{F}_2$  system seems to negate the details of such a description.

The fact that the fracton model (in the sense of overdamped excitation modes) is not a useful model for the interpretation of either the isotropic or the anisotropic  $d=3$  systems well away from the percolation threshold leaves one with doubts about the validity of the model in the weakly anisotropic system  $\text{Mn}_{0.5}\text{Zn}_{0.5}\text{F}_2$ , despite the position taken in the work of Uemura and Birgeneau.<sup>11</sup> To see fracton behavior at a concentration that is twice the percolation threshold concentration, as was claimed, would in fact be quite surprising. At such a high magnetic concentration almost no fractal-like structure exists. It would be of considerable interest to study the  $\text{Mn}_x\text{Zn}_{1-x}\text{F}_2$  system much closer to the percolation threshold. One may well see the apparent damping lessen as one approaches the percolation threshold concentration. The observed behavior could prove to be compatible with that observed in the  $\text{Fe}_x\text{Zn}_{1-x}\text{F}_2$  system studied here. Since the anisotropy in  $\text{Mn}_x\text{Zn}_{1-x}\text{F}_2$  system is dipolar, it becomes random in strength and direction upon dilution. Hence, although the excitations would be expected to be more separated than in the anisotropic case, the intrinsic widths may be larger and, hence, tend to obscure the structure. This may explain the difficulty in resolving structure in this system, though some detailed structure was observed in the experiments in a previous study by Dietrich *et al.*<sup>22</sup> at a concentration  $x=0.68$ . It is difficult to compare the observed line shape in  $\text{Mn}_{0.5}\text{Zn}_{0.5}\text{F}_2$  with the cluster model for the overall position, width and relative amplitude as a function of  $q$ , since the effective anisotropy and exchange interaction strengths in the  $\text{Mn}_x\text{Zn}_{1-x}\text{F}_2$  upon dilution are not well known. Nevertheless, the general behavior observed in  $\text{Mn}_{0.5}\text{Zn}_{0.5}\text{F}_2$  is not inconsistent with the cluster model in a weakly anisotropic system. The magnon at  $q=0$  could be spreading into several localized peaks with some intrinsic width at  $q>0$ . The overall width is expected to be

larger than in  $\text{Fe}_x\text{Zn}_{1-x}\text{F}_2$  because the anisotropy is much weaker.

Very recently, evidence for fracton behavior has been observed<sup>23</sup> in the dilute Heisenberg antiferromagnet  $\text{RbMn}_{0.39}\text{Mg}_{0.61}\text{F}_3$ , with a concentration quite close to the percolation threshold  $x_p=0.31$ . In this case, a broad background upon which the cluster model excitations are observed, has been shown to exhibit properties predicted from computer simulations<sup>24</sup> and the single length scale postulate.<sup>12</sup> This confirms that such fracton behavior can only be expected very close to the percolation threshold.

Clearly, a more profound theoretical basis for understanding the excitations in diluted magnetic systems is greatly needed, in particular for systems with significant anisotropy. There is no detailed understanding of the partial success of the simple cluster model and none at all of the three-peak structure indicated by the present measurements. On the experimental side, more extensive measurements of the detailed excitation spectrum at other concentrations is needed for the  $\text{Fe}_x\text{Zn}_{1-x}\text{F}_2$  system to verify whether the three-peak structure is a common feature for all concentrations. As mentioned above, detailed measurements at other concentrations are needed in the  $\text{Mn}_x\text{Zn}_{1-x}\text{F}_2$  system to indicate whether a more suitable description than the damped fracton one given previously can be experimentally constructed. If one is to observe fracton effects, concentrations much closer to the percolation threshold must be studied.

We would like to thank H. Ikeda and J. A. Fernandez-Baca for helpful discussions and suggestions and for describing their results prior to publication. This research was supported in part by the Division of Materials Sciences, U.S. Department of Energy, under Contract No. De-AC05-84OR21400 with Martin Marietta Energy Systems, Inc. and in part by Department of Energy Grant No. De-FG03-87ER45324. C. Paduani would like to thank the Brazilian agency CAPES for support during his stay in the U.S.

\*Present address: Departamento de Física, Universidade Federal de Santa Catarina, Campus, Tindade, CEP 88040-900 Florianopolis, Santa Caterina, Brazil.

<sup>1</sup>Y. Imry and S.-k. Ma, *Phys. Rev. Lett.* **35**, 1399 (1975).

<sup>2</sup>S. Fishman and A. Aharony, *J. Phys. C* **12**, L729 (1979).

<sup>3</sup>J. Cardy, *Phys. Rev. B* **29**, 505 (1984); A. R. King and D. P. Belanger, *J. Magn. Magn. Mater.* **54-57**, 19 (1986); D. P. Belanger, A. R. King, and V. Jaccarino, *Appl. Phys.* **55**, 2383 (1984).

<sup>4</sup>J. B. M. da Cunha, J. H. de Araujo, L. Amaral, A. Vasquez, J. T. Moro, F. C. Montenegro, S. M. Rezende and M. D. Coutinho-Filho, *Hyperfine Interact.* **54**, 489 (1990).

<sup>5</sup>C. L. Henley, *Phys. Rev. Lett.* **54**, 2030 (1985).

<sup>6</sup>D. P. Belanger and H. Yoshizawa, *Phys. Rev. B* **47**, 5051 (1993).

<sup>7</sup>E. F. Shender, *Zh. Eksp. Teor. Fiz.* **75**, 352 (1978) [*Sov. Phys. JETP* **48**, 175 (1978)]; *J. Phys. C* **9**, L309 (1976).

<sup>8</sup>A. Aharony, S. Alexander, O. Entin-Wohlman, and R. Orbach,

*Phys. Rev. B* **31**, 2565 (1985); *Phys. Rev. Lett.* **58**, 132 (1987).

<sup>9</sup>G. Polatssek, O. Entin-Wohlman, and R. Orbach, *Phys. Rev. B* **39**, 9353 (1989).

<sup>10</sup>R. Orbach and Kin-Wah Yu, *J. Appl. Phys.* **61**, 3689 (1987).

<sup>11</sup>Y. J. Uemura and R. J. Birgeneau, *Phys. Rev. B* **36**, 7024 (1987).

<sup>12</sup>T. Nakayama, K. Yakubo, and R. Orbach, *Rev. Mod. Phys.* (to be published).

<sup>13</sup>M. T. Hutchings, B. D. Rainford, and H. J. Guggenheim, *J. Phys. C* **3**, 307 (1970).

<sup>14</sup>G. K. Wertheim, D. N. E. Buchanan, and H. J. Guggenheim, *Phys. Rev.* **152**, 527 (1966).

<sup>15</sup>Cid B. de Araujo, *Phys. Rev. B* **22**, 266 (1980).

<sup>16</sup>A. R. King, V. Jaccarino, T. Sakakibara, M. Motokawa, and M. Date, *Phys. Rev. Lett.* **47**, 117 (1981).

<sup>17</sup>G. J. Coombs, R. A. Cowley, W. J. L. Buyers, E. C. Svensson, T. M. Holden, and D. A. Jones, *J. Phys. C* **9**, 2167 (1976).

<sup>18</sup>R. A. Cowley, O. W. Dietrich, and D. A. Jones, *J. Phys. C* **8**,

- 3023 (1975).
- <sup>19</sup>I. Ya. Korenblit and E. F. Shender, *Phys. Rev. B* **48**, 9478 (1993).
- <sup>20</sup>M. Takahashi and H. Ikeda, *Phys. Rev. B* **47**, 9132 (1993).
- <sup>21</sup>H. Ikeda and K. Ohoyama, *Phys. Rev. B* **45**, 7484 (1992).
- <sup>22</sup>O. W. Dietrich, G. Meyer, R. A. Cowley, and G. Shirane, *Phys. Rev. Lett.* **35**, 1735 (1975).
- <sup>23</sup>H. Ikeda, J. A. Fernandez-Baca, R. M. Nicklow, M. Takahashi, and K. Iwasa (unpublished).
- <sup>24</sup>K. Yakubo, T. Terao, and T. Nakayama (unpublished).